Communications in Computational Chemistry
Commun. Comput. Chem., Vol. 7, No. 1, 81–87
doi: 10.4208/cicc.2025.84.02
Regular Article

Enhancing Optoelectronic Properties of Quasi-2D Ruddlesden–Popper Perovskites via Pseudo–Halogen Doping: A First–Principles Study on $Cs_2Pb(SCN)_2Br_2$

Peng Xiong[1,2,3,†], Jia-Ming Li[1,2,†], Zhi-Mi Zhang[3], Zhong-Yuan Wang[3], Jian Wu[1,2,*]

and Chuan-Jia Tong[3,*]

[1] *International Institute for Materials Innovation, Nanchang University, Nanchang, 330031, China;*

[2] *School of Physics and Materials Science, Nanchang University, Nanchang, 330031, China;*

[3] *Institute of Quantum Physics, Hunan Key Laboratory of Nanophotonics and Devices, Hunan Key Laboratory of Super-Microstructure and Ultrafast Process, School of Physics, Central South University, Changsha 410083, China.*

[*] Corresponding authors: wujian@ncu.edu.cn (J. Wu), chuanjia.tong@csu.edu.cn (C.-J. Tong).

Received on 15 March 2025; Accepted on 11 April 2025

[†]: Peng Xiong and Jia-Ming Li contributed equally to this work.

Abstract

Two-dimensional (2D) Ruddlesden–Popper (RP) perovskites have been intensively investigated due to their superior stability and outstanding optoelectronic properties. Although A-site doping in quasi–2D RP–phase perovskites has been extensively studied, the effect of X–site doping remains unknown. Using first–principles calculations, this work demonstrates that SCN^- substitution in $Cs_2Pb(SCN)_2Br_2$ induces a structural transformation from isotropic to anisotropic through octahedral tilting along the b-axis, reducing octahedral spacing from 5.17 to 4.88 Å. This structural modification enhances carrier mobility, dramatically increases exciton binding energy from 30.47 to 145.39 meV, and improves defect tolerance compared to pristine Cs_2PbBr_4. These modifications synergistically suppress non-radiative recombination pathways while promoting radiative processes, so that improve its performance as a promising light–emitting diode (LED) material. These findings establish pseudo–halogen substitution as a promising strategy for optimizing carrier transport and radiative efficiency in low-dimensional perovskite LED devices.

Key words: Ruddlesden–Popper (RP) perovskites, LED, exciton binding energy, carrier mobility.

All–inorganic three–dimensional perovskites ABX_3 exhibit remarkable optoelectronic properties [1-8], achieving external quantum efficiencies (EQE) up to 32% in perovskite light–emitting diodes (PeLEDs) applications [9]. However, fundamental limitations arise from their inherently weak exciton binding energy (E_b) and structural instability [10-12]. The slow radiative (bimolecular)

recombination rate in three–dimensional perovskites frequently results in free carriers (FCs) being captured by defects, leading to non–radiative recombination instead of radiative decay [13]. Two–dimensional (2D) and quasi–2D perovskites effectively address these limitations through quantum confinement effects, which enhance E_b and improve structural stability through reduced dimensionality [14-16]. A critical factor governing the light–emitting diode (LED) performance of quasi–2D perovskites is the competition between radiative and non–radiative recombination channels, which is intrinsically linked to carrier mobility, E_b, and defect formation energy.

Layered lead halide perovskites have recently garnered attention due to their tunable optoelectronic properties and improved stability [16-18]. For example, $Cs_2Pb(SCN)_2Br_2$, a pseudo–halogen–doped 2D Ruddlesden–Popper (RP) perovskite, exhibits enhanced stability and quantum confinement effects [19-21]. Recent experimental investigations have established the fundamental properties and applications of the materials: Liao *et al.* successfully synthesized single crystal $Cs_2Pb(SCN)_2Br_2$ by the antisolvent vapor–assisted crystallization (AVC) method [22]. While Liu *et al.* prepared quasi–2D RP–phase perovskite $Cs_2Pb(SCN)_2Br_2$ polycrystalline wafer, and investigated its potential in X–ray detection [23]. Despite the promising photovoltaic properties demonstrated by this material, the fundamental mechanisms underlying their performance remain incompletely understood, especially the influence of pseudo–halogen doping in $Cs_2Pb(SCN)_2Br_2$. Specifically, the impact of such doping on radiative and non-radiative recombination processes requires further elucidation. Therefore, further theoretical research is needed to understand the microscopic mechanisms by which pseudo–halogen doping affects perovskite performance.

In this work, the $Cs_2Pb(SCN)_2Br_2$ and Cs_2PbBr_4 systems are presented as a comparative analysis to elucidate the influence of pseudo–halogen doping on their optoelectronic properties. Through first–principles calculations, we investigate the electronic structure, E_b, carrier mobility, and defect formation energetics. Our results indicate that SCN^- modifies the crystal structure, improves the structure stability, suppresses non–radiative pathways, and enhances carrier mobility. These improvements are attributed to reduced defect formation energies and optimized E_b, which collectively enhance radiative efficiency. The results establish pseudo–halogen engineering as a viable strategy for enhancing perovskite optoelectronic properties, offering a framework for designing high–performance LEDs.

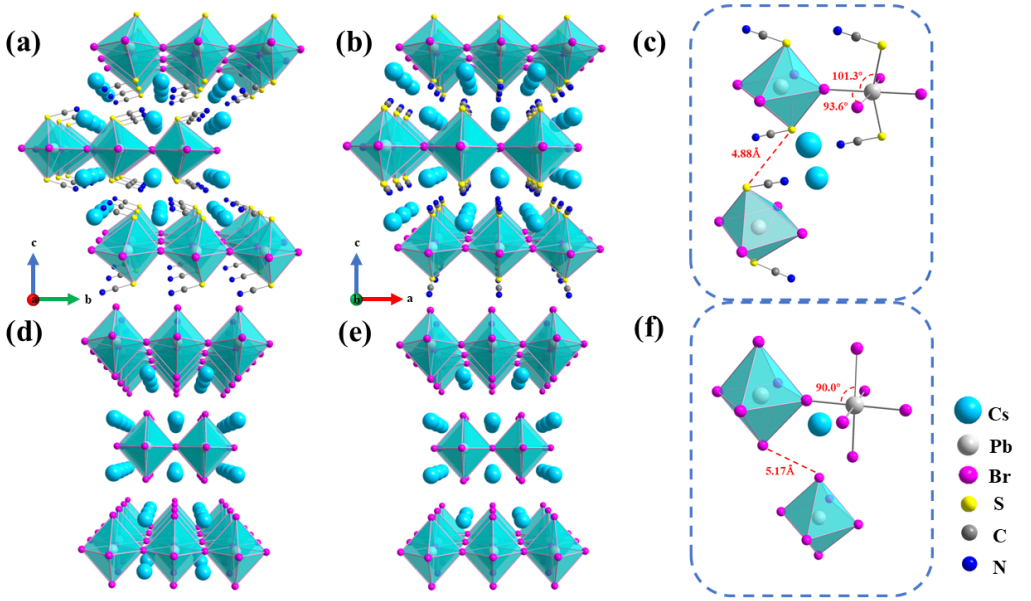

Figure 1. (a) Front view and (b) side view of the $Cs_2Pb(SCN)_2Br_2$. (c) Schematic of the octahedral distortion angle and octahedral spacing of the $Cs_2Pb(SCN)_2Br_2$. (d) Front and (e) side view of the Cs_2PbBr_4. (f) The schematic of the octahedral distortion angle and octahedral spacing of the Cs_2PbBr_4. The blue spheres represent Cs atoms, the white spheres represent Pb atoms, the purple spheres represent Br atoms, the yellow spheres represent S atoms, the grey spheres represent C atoms and the dark blue spheres represent N atoms.

The electronic structure and electronic properties were obtained using density functional theory (DFT) as implemented in the Vienna *ab initio* simulation package (VASP) [24-27]. The exchange–correlation energy was modeled using the generalized gradient approximation (GGA) with the Perdew–Burke–Ernzerhof (PBE) functional[28-30]. To accurately account for van der Waals (vdW) interactions, the Grimme DFT-D3 method with Becke–Johnson damping was employed [31-33]. All calculations were performed on a $2 \times 2 \times 2$ supercell, with a plane–wave cutoff energy of 500 eV. The optimization was carried out using a $2 \times 2 \times 1$ *k*–point mesh until the energy converged to 10^{-5} eV. Additionally, all atomic positions were relaxed until the maximum residual force on each atom was reduced to less than 0.01 eV/Å.

According to the deformation potential (DP) theory introduced by Bardeen and Shockley [34-35], the carrier mobility in crystalline materials is expressed by the following equation:

$$\mu_\beta^{3D} = \frac{e\langle\tau_\beta\rangle}{m^*} = \frac{2\sqrt{2\pi}eC_\beta^{3D}\hbar^4}{3(\kappa_B T)^{3/2}E_\beta^{3D}m^{*5/2}} \quad (1)$$

where e is the electron charge, $\hbar$ is the approximate Planck constant, k_B is the Boltzmann constant, and T is the room temperature ($T = 300$ K). m^* is the effective mass. C_β^{3D} denotes the elastic modulus of the crystal along the transport direction, and E_β^{3D} denotes the deformation potential constant along the transport direction for holes at the valence band maximum (VBM) or for electrons at the conduction band minimum (CBM).

In this study, the Delta–Self–Consistent Field (ΔSCF) method [36-38] was employed to calculate the E_b. An electron is excited from the VBM to the CBM, and then the orbital positions are fixed